

RESEARCH ARTICLE

On stream selection for interference alignment with limited feedback in heterogeneous networks

Esra Aycan Beyazıt^{1*}, Berna Özbek¹ and Didier Le Ruyet²¹ Electrical and Electronics Engineering Department, Izmir Institute of Technology, Izmir, Turkey² Research lab CEDRIC/LAETITIA, Conservatoire National Des Arts et Métiers, Paris, France

ABSTRACT

This paper presents a stream selection based interference alignment approach with imperfect channel state information for heterogeneous networks. The proposed solution constructs stream sequences by selecting only the strongest stream of each user where the first stream of the constructed stream sequences is associated to a pico user. While selecting the streams, the channel matrices of the unselected streams are projected orthogonally to the virtual transmit and receive channels of the selected stream in order to align the interference in the null space of these virtual channels. In addition, the influence of imperfect channel state information on the proposed algorithm is analysed. A bit allocation scheme is given by deriving an upper bound on the rate loss because of quantisation. The simulation results are carried out by considering various scenarios with different locations of pico cells at the cell edge regions of the macro cell. The performance results show that the proposed algorithm with the imperfect channel state information achieves higher performance than the existing algorithms. Copyright © 2016 John Wiley & Sons, Ltd.

*Correspondence

Esra Aycan Beyazıt, Electrical and Electronics Engineering Department, Izmir Institute of Technology, Izmir, Turkey.

E-mail: aycanesra@gmail.com

Received 24 February 2016; Revised 27 May 2016; Accepted 19 June 2016

1. INTRODUCTION

Future wireless networks require more spectral efficiency and larger coverage area because of the increasing demand on the wireless services. Therefore, heterogeneous networks are considered as a promising technique for cellular networks while they provide a deployment of large number of smaller cells with different transmit power levels in the coverage of the conventional macro cell. Thus, the traffic load on the macrocell can be offloaded to the small cells, and the poor coverage areas of the macro cell can be enhanced, such as cell-edge regions. In addition, co-channel deployment among small and macro cells is commonly applied to increase the spectral efficiency [1].

Despite the advantages of the heterogeneous networks, dense deployment of small cells increases the effect of the co-channel interference [2]. It is possible to handle the interference in the heterogeneous networks using different approaches [3, 4]. Interference alignment (IA) is one of the techniques to effectively mitigate the interference in wireless networks [5]. It is introduced as a linear precoding technique that aligns the interfering signals in time, frequency or space. The key idea is to align the interfering signals into one dimensional subspace at each receiver

by designing precoding and postcoding vectors so that the desired signal can be obtained in the interference-free signal subspaces.

Interference alignment studies first started to manage the interference using symbol extensions in K pair interference channels, and it has been shown that the capacity of the network linearly grows without any bound as the network size increases using the symbol extension method [6]. Different approaches have been developed to solve the IA problem. Closed form solutions for the IA problem are difficult to obtain for large scale networks; therefore, for practical systems, iterative and distributed IA approaches have been intensively studied [7]. In addition, stream selection based approaches have been presented in [8] where the least interfering streams are selected to be in the null space of the previously selected ones. The IA approaches have been extended for cellular networks [9–11]. Besides, IA has also been studied for heterogeneous networks to handle the problems caused by the coexistence of macro and small cells [12–15].

The studies mentioned earlier assume that the channel state information (CSI) is available at all transmitters and receivers. Thus, the interference can be perfectly aligned by designing the precoders and postcoders. Because this

assumption is not realistic for practical systems, two methods have been implemented to get the CSI, which are reciprocity and feedback. Because reciprocity is not possible to implement for frequency division duplexing systems, feedback schemes have been commonly implemented in cellular networks [16]. In the feedback mechanism, receivers estimate the channel coefficients by using training sequences. After the channel estimation, receivers feedback the quantised CSI in a centralised or a distributed topology to the transmitters with a certain number of bits using codebooks known at both the transmitters and the receivers. Thus, the precoders and postcoders can be calculated to align the interference. The quality of the obtained CSI by the limited feedback affects the performance of the IA. As the size of the codebook increases, the distortion caused by the limited feedback decreases, but the feedback overhead increases in the network. Therefore, the number of bits for CSI should be optimised depending on the channel conditions [17].

Equal bit allocation in which the number of feedback-bits for each channel is fixed is not efficient for heterogeneous networks because of different pathloss and shadowing effects. In [18], equal bit allocation has been studied on the stream selection based IA approach, which selects multiple streams for each user comparing different distortion metrics using random vector quantisation (RVQ). However, the optimal number of streams has been investigated for the performance of IA with limited channel direction information (CDI) feedback, and it has been stated that the single data stream for each user-base station (BS) pair is optimal because of the intra-stream interference problem in the multiple streams transmission [19].

In order to increase the system throughput with the quantised channel, different feedback bit allocation schemes have been studied for the IA in K pair multiple-input-multiple-output (MIMO) systems. In order to minimise the effect of the distortion, an adaptive feedback bit allocation scheme that adaptively selects the number of feedback bits to the links of each transmitter-receiver pair have been designed [20]. In the context of the heterogeneous networks, optimising the bit allocation can increase the performance of the feedback schemes for IA technique by considering the distinctive features of the heterogeneous networks, such as unequal number of transmit antennas and transmit power levels [21, 22].

In the study of [15], stream sequences have been constructed where users can have multiple streams assuming the availability of the perfect CSI at the transmitters. In this paper, we propose a novel stream selection based IA algorithm for the heterogeneous networks with imperfect CSI to improve the performance by presenting an adaptive feedback bit allocation scheme. The proposed algorithm selects a stream sequence from a predetermined set of sequences having a regular structure in which the first stream is associated to a pico user because the average signal to noise ratio (SNR) of the pico users is higher than the macro user. To prevent the intra-stream interference and to decrease the quantisation error in the limited feedback systems, a

single stream is selected for each user in the proposed algorithm. Among the constructed stream combinations, the one achieving the highest sum-rate is chosen. An adaptive feedback bit allocation scheme is designed to maximise the overall capacity for the proposed IA scheme.

The contributions of this paper can be summarised as follows:

- A novel stream selection based IA algorithm is proposed for imperfect CSI considering the properties of the heterogeneous networks.
- An adaptive feedback bit allocation scheme is presented for the proposed algorithm in order to increase the system throughput for a fixed feedback load per user.

The rest of this paper is organised as follows. The system model and the channel quantisation scheme are presented in Section 2. The IA method based on the stream selection for heterogeneous networks is proposed in Section 3. An adaptive bit allocation method is presented in Section 4. In Section 5, the performance evaluations are given, and the study is concluded in Section 6.

Notations: Rank(\mathbf{A}) refers to the rank of the matrix \mathbf{A} ; $(\mathbf{A})^H$ represents the transpose conjugate of the matrix \mathbf{A} . Capital greek letters such as Ω denote sets, and $|\Omega|$ denotes the number of elements in Ω .

2. SYSTEM MODEL

In this study, a K pair heterogeneous network composed of $K - 1$ pico BSs and one macro BS with N_{T_k} transmitter and N_{R_k} receiver antennas is considered as shown in Figure 1. For the sake of simplicity, macro BS–macro user pair is determined by the pair $k = 1$, and pico BS–pico user pairs are kept in the set $\Gamma = \{2, \dots, K\}$.

2.1. Transmission model

The received signal at user k is defined as follows:

$$\mathbf{y}_k = \sqrt{P_k} \alpha_{kk} \mathbf{H}_{kk} \tilde{\mathbf{T}}_k \mathbf{s}_k + \sum_{\substack{j=1, \\ j \neq k}}^K \sqrt{P_j} \alpha_{kj} \mathbf{H}_{kj} \tilde{\mathbf{T}}_j \mathbf{s}_j + \mathbf{n}_k \quad (1)$$

where $\alpha_{kj} \mathbf{H}_{kj}$ is the channel matrix between the j^{th} transmitter and the k^{th} receiver with dimension $N_{R_k} \times N_{T_j}$. Each element of \mathbf{H}_{kj} includes fading modelled as an independent and identically distributed complex Gaussian random variable with $\mathcal{CN}(0, 1)$. α_{kj} denotes the pathloss and shadowing. For each receiver k , \mathbf{n}_k is a $N_{R_k} \times 1$ vector. Each element of \mathbf{n}_k represents additive white Gaussian noise with zero mean and variance of σ^2 . P_k is the transmit power of the k^{th} BS. $\tilde{\mathbf{T}}_k$ is the unitary precoding matrix of the k^{th} transmitter with dimension $N_{T_k} \times q_k$, and it is obtained by the proposed algorithms under the quantised channel, $\tilde{\mathbf{H}}_{kj}$, between the j^{th} transmitter and the k^{th} receiver with dimension $N_{R_k} \times N_{T_j}$. The k^{th} transmitter has q_k independent streams with $q_k \leq d_k$ where $d_k = \min(N_{R_k}, N_{T_k})$. \mathbf{s}_k

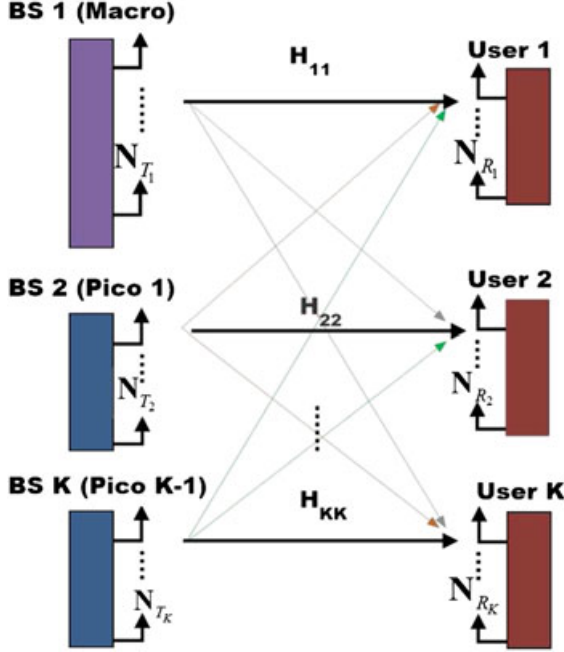


Figure 1. System model for MIMO heterogeneous network.

is the symbol vector with dimension of $q_k \times 1$ and denoted as $\mathbf{s}_k = [s_{k,1} \dots s_{k,q_k}]^T$ where $\mathbb{E}[\|\mathbf{s}_k\|^2] = 1$.

Each user decodes the received signals by multiplying them with the postcoding vectors, $\tilde{\mathbf{D}}_k$, of dimension $N_{R_k} \times q_k$, and they are obtained by the proposed algorithms under the quantised channel. Thus, the decoded data symbols are given as $\hat{\mathbf{y}}_k = \tilde{\mathbf{D}}_k^H \mathbf{y}_k$.

The achievable data rate of user k can be expressed as follows:

$$\tilde{R}_k = \log_2(1 + \tilde{\gamma}_k) \quad (2)$$

where $\tilde{\gamma}_k$ is the signal to interference noise ratio (SINR) of the k^{th} user, and it is given by

$$\tilde{\gamma}_k = \frac{P_k \alpha_{kk} \tilde{\mathbf{d}}_k^H \mathbf{H}_{kk} \tilde{\mathbf{t}}_k \tilde{\mathbf{t}}_k^H \mathbf{H}_{kk}^H \tilde{\mathbf{d}}_k}{\tilde{\mathbf{d}}_k^H \tilde{\mathbf{B}}_k \tilde{\mathbf{d}}_k}, \quad k = 1, \dots, K \quad (3)$$

where $\tilde{\mathbf{t}}_k$ is the k^{th} column vector of $\tilde{\mathbf{T}}_k$ with the size of $N_{T_k} \times 1$ and $\tilde{\mathbf{d}}_k$ is the k^{th} column vector of $\tilde{\mathbf{D}}_k$ with the size of $N_{R_k} \times 1$. The interference plus noise covariance matrix of the k^{th} receiver, $\tilde{\mathbf{B}}_k$, is defined as

$$\tilde{\mathbf{B}}_k = \sum_{j=1, j \neq k}^K P_j \alpha_{kj} \mathbf{H}_{kj} \tilde{\mathbf{t}}_j \tilde{\mathbf{t}}_j^H \mathbf{H}_{kj}^H + \sigma^2 \mathbf{I}_{N_{R_k}}, \quad k = 1, \dots, K \quad (4)$$

The achievable sum rate is calculated as follows:

$$\tilde{S}R = \sum_{k=1}^K \tilde{R}_k \quad (5)$$

Because the perfect CSI is not available at the transmitters, the quantised CSI is considered throughout this study.

The main objective is to mitigate the interference while finding the best stream sequence. The stream sequence, which maximises the total sum rate of the network while guaranteeing that at least one stream is chosen from each user can be formulated as follows:

$$\{(\tilde{\mathbf{T}}_k^*, \tilde{\mathbf{D}}_k^*)\}_{k=1, \dots, K} = \underset{\tilde{\mathbf{T}}_k, \tilde{\mathbf{D}}_k}{\text{argmax}} \tilde{S}R \quad (6a)$$

$$\text{s.t. } q_k = 1 \quad k = 1, \dots, K \quad (6b)$$

2.2. Channel quantisation model

In this section, a limited feedback scheme is presented based on RVQ. The proposed IA algorithm requires all the CSI to compute all precoding and postcoding vectors. Therefore, a centralised feedback model is considered in which the macro BS collects all the CSIs from pico BSs through the error and delay free backhaul links. Each step of the feedback scheme can be explained as follows:

- Step 1: It is assumed that the CSI has been perfectly known at each receiver as $\mathbf{H}_{kj} = \tilde{\mathbf{H}}_{kj} \times \|\mathbf{H}_{kj}\|_F$ where $\tilde{\mathbf{H}}_{kj}$ is the CDI. Each CDI is calculated by normalising the channel matrix between the j^{th} transmitter and the k^{th} receiver using its Frobenius norm as $\tilde{\mathbf{H}}_{kj} = \frac{\mathbf{H}_{kj}}{\|\mathbf{H}_{kj}\|_F}$.
- Step 2: Each receiver quantises its CDI belonging to the desired and the interfering BS. In order to quantise each CDI, codebooks are generated by using RVQ, which contains $2^{B_{kj}}$ codewords, where B_{kj} is the number of quantisation bits to quantise the channel between the j^{th} transmitter and the k^{th} receiver. The codewords are independent and isotropically distributed over the unit sphere.

The normalised channel matrix, $\tilde{\mathbf{H}}_{kj}$, $\forall k, \forall j$, is vectorized as $\tilde{\mathbf{h}}_{kj} = \text{vec}(\tilde{\mathbf{H}}_{kj})$ where $\tilde{\mathbf{h}}_{kj} \in \mathbb{C}^{N_{T_j} N_{R_k} \times 1}$.

The codebook is generated using RVQ as $\mathbf{W}_{kj} = \{\mathbf{c}_{kj}^1 \dots \mathbf{c}_{kj}^i \dots \mathbf{c}_{kj}^{2^{B_{kj}}}\}$ where $\|\mathbf{c}_{kj}^i\| = 1, \forall i$ and $\mathbf{c}_{kj}^i \in \mathbb{C}^{N_{T_j} N_{R_k} \times 1}$.

The codeword \mathbf{c}_{kj}^{i*} that minimises the Chordal distance metric is selected as the quantised CDI, $\tilde{\mathbf{h}}_{kj} = \mathbf{c}_{kj}^{i*}$. The Chordal distance is calculated as follows:

$$\mathbf{c}_{kj}^{i*} = \min d_c(\tilde{\mathbf{h}}_{kj}, \mathbf{c}_{kj}^i) \quad (7)$$

where $d_c(\tilde{\mathbf{h}}_{kj}, \mathbf{c}_{kj}^i) = \sqrt{1 - |\tilde{\mathbf{h}}_{kj}^H \mathbf{c}_{kj}^i|^2}$. The selected codeword, \mathbf{c}_{kj}^{i*} , can also be called quantised unit vector channel and denoted as $\tilde{\mathbf{h}}_{kj}$.

- Step 3: The indices of the selected codewords are fed back to the associated transmitters through feedback links.

- Step 4: Each pico BS receives the codebook indices and sends them to the macro BS through the backhaul links.
- Step 5: The macro BS reconstructs CSIs by using the codebooks known at both sides as follows. First, $\tilde{\mathbf{h}}_{kj}$ is reshaped as $\tilde{\mathbf{H}}_{kj} \in \mathbb{C}^{N_{R_k} \times N_{T_j}}$. Accordingly, the quantised channel, $\tilde{\mathbf{H}}_{kj}$, is calculated as $\tilde{\mathbf{H}}_{kj} = \tilde{\mathbf{H}}_{kj} \times \|\mathbf{H}_{kj}\|_F$. After the CSIs are reconstructed, the precoding and postcoding vectors are computed by implementing the proposed algorithm.
- Step 6: The macro BS distributes the precoding and the postcoding vectors to the pico BSs.
- Step 7: Each transmitter forwards the postcoders to the corresponding receivers using the forward link.

The quantisation error caused by RVQ can be modelled as follows [20, 23]:

$$\begin{aligned} \tilde{\mathbf{h}}_{kk} &= \cos \theta_{kk} \bar{\mathbf{h}}_{kk} + \sin \theta_{kk} \mathbf{z}_{kk} \\ &= \sqrt{1 - e_{kk}} \bar{\mathbf{h}}_{kk} + \sqrt{e_{kk}} \mathbf{z}_{kk} \end{aligned} \quad (8)$$

where θ_{kk} is the angle between $\bar{\mathbf{h}}_{kk}$ and $\tilde{\mathbf{h}}_{kk}$ and $e_{kk} \triangleq \sin^2(\theta_{kk})$. \mathbf{z}_{kk} is the unit vector representing the direction of the quantisation error vector, and it is isotropically distributed in the null space of $\bar{\mathbf{h}}_{kk}$. e_{kk} is the minimum of $2^{B_{kk}}$ independent $\beta((N_{T_k} N_{R_k} - 1), 1)$ random variables [24]. Accordingly, Equation (8) can be expressed in matrix form using the channel matrix as follows:

$$\begin{aligned} \tilde{\mathbf{H}}_{kk} &= \cos \theta_{kk} \bar{\mathbf{H}}_{kk} + \sin \theta_{kk} \mathbf{Z}_{kk} \\ &= \sqrt{1 - e_{kk}} \bar{\mathbf{H}}_{kk} + \sqrt{e_{kk}} \mathbf{Z}_{kk} \end{aligned} \quad (9)$$

where $\mathbf{Z}_{kk} \in \mathbb{C}^{N_{R_k} \times N_{T_k}}$ is reshaped as matrix using the vector $\mathbf{z}_{kk} \in \mathbb{C}^{N_{R_k} N_{T_k} \times 1}$.

In order to generate values for $Z = e_{kk}$, the following cumulative distribution function can be used in inverse transform sampling [24].

$$F_Z(z) = P(Z \leq z) = 1 - \left(1 - z^{N_{R_k} N_{T_k} - 1}\right)^{2^{B_{kk}}} \quad (10)$$

3. K-STREAM SELECTION ALGORITHM

In this section, the proposed algorithm, K-Stream Selection is described. The KSS algorithm selects a stream sequence from a predetermined set of sequences having a regular structure. For each stream in each stream sequence, the generated interference between the selected and the unselected streams is mitigated by performing orthogonal projections. Because the process of the projections is performed at each stream selection, the IA procedure is explained before presenting the selection procedure of the KSS algorithm as follows.

3.1. Interference alignment procedure

In stream selection based IA algorithms, each stream is selected in the null space of the previously selected streams

where streams are computed from the singular value decomposition (SVD) of all the channels, $(\alpha_{kk} \tilde{\mathbf{H}}_{kk}) = \tilde{\mathbf{U}}_k \tilde{\mathbf{S}}_k \tilde{\mathbf{V}}_k^H$. The l^{th} column vector of $\tilde{\mathbf{V}}_k$ and $\tilde{\mathbf{U}}_k$ is denoted as $\tilde{\mathbf{v}}_k^l$ and $\tilde{\mathbf{u}}_k^l$, respectively. The interference is aligned after each stream selection step using orthogonal projections.

When a stream is selected, there are two kinds of interference generated between the selected and the unselected streams. The first one is the interference from the selected stream to the unselected streams, and the second one is the interference to the selected stream from the unselected streams. Therefore, two types of virtual channels are defined as Virtual Receiving Channels (VRCs) and Virtual Transmitting Channels (VTCs) [8]. These can be expressed as follows:

- Virtual Receiving Channel: VRC is the channel between the transmitter k and the receiver k^* including the postcoding vector of the selected stream l^* , $\tilde{\mathbf{u}}_{k^*}^{l^*}$.

$$\text{VRC}_{k^*k}^{l^*} = \left(\tilde{\mathbf{u}}_{k^*}^{l^*}\right)^H \tilde{\mathbf{H}}_{k^*k} \quad (11)$$

- Virtual Transmitting Channel: VTC is the channel between the transmitter k^* and the receiver k including the precoding vector of the selected stream l^* , $\tilde{\mathbf{v}}_{k^*}^{l^*}$.

$$\text{VTC}_{kk^*}^{l^*} = \tilde{\mathbf{H}}_{kk^*} \tilde{\mathbf{v}}_{k^*}^{l^*} \quad (12)$$

For each selected stream, multiple VRCs and VTCs are designed by using the precoder and decoder vectors, respectively. These vectors are obtained from the SVD procedure. Precoding and postcoding matrices are constructed from the precoding and postcoding vectors corresponding to the selected streams, and they are expressed as $\tilde{\mathbf{T}}_{k^*} = [\tilde{\mathbf{v}}_{k^*}^1, \tilde{\mathbf{v}}_{k^*}^2, \dots, \tilde{\mathbf{v}}_{k^*}^{q_k}]$ and $\tilde{\mathbf{D}}_{k^*} = [\tilde{\mathbf{u}}_{k^*}^1, \tilde{\mathbf{u}}_{k^*}^2, \dots, \tilde{\mathbf{u}}_{k^*}^{q_k}]$, respectively.

Therefore, after the virtual channels of user k^* are obtained, the impact of the selected stream of user k^* to the unselected streams is reduced by orthogonal projections. More precisely, the space spanned by the unselected potential precoding and postcoding of each user $k \neq k^*$ is projected orthogonally to the corresponding VRC and VTC of the selected stream l^* belonging to user k^* . Projected matrices are denoted by $\tilde{\mathbf{H}}_{kk}^\perp$ and, initially, $\tilde{\mathbf{H}}_{kk}^\perp = \tilde{\mathbf{H}}_{kk}$. The orthogonal projection matrix parallel to vector \mathbf{x} is calculated as $\mathbf{P}_x^\perp = \mathbf{I} - \frac{\mathbf{x}\mathbf{x}^H}{\|\mathbf{x}\|^2}$.

The vectors of the projected matrices $\tilde{\mathbf{H}}_{kk}^\perp$, $\forall k \neq k^*$, are in the null space of all previously selected streams. At each stream i , the interference from the unselected streams to the selected stream is reduced by projecting the channel matrices $\tilde{\mathbf{H}}_{kk}^\perp$ orthogonally to the VRC, and the interference to the unselected streams from the selected stream is reduced by projecting the channel matrices $\tilde{\mathbf{H}}_{kk}^\perp$ orthogonally to the VTC. The reason for projecting all VTCs and VRCs of the unselected streams can be explained as follows. At the beginning, all streams are available for the selection. When

a stream is selected, all channels of the unselected streams are orthogonally projected to both VTC and VRC of the selected stream. In this way, when another stream is to be selected, its channel is guaranteed to become orthogonal to the channels of the previously selected streams, and thus, it does not generate any interference to them.

Algorithm 1 Interference Alignment Algorithm

Input: α_{kk} , $\tilde{\mathbf{H}}_{kk}^\perp$, $\tilde{\mathbf{H}}_{kk^*}$ and $\tilde{\mathbf{H}}_{k^*k}$ $\forall k$; $\tilde{\mathbf{v}}_{k^*}^{l^*}$, $\tilde{\mathbf{u}}_{k^*}^{l^*}$, $\tilde{\mathbf{T}}_{k^*}$, $\tilde{\mathbf{D}}_{k^*}$
 Project orthogonally to VRC, $\tilde{\mathbf{u}}_{k^*}^{l^*H} \tilde{\mathbf{H}}_{k^*k^*}$
 $\tilde{\mathbf{H}}_{kk}^\perp = \tilde{\mathbf{H}}_{kk}^\perp \mathbf{P}_{\tilde{\mathbf{u}}_{k^*}^{l^*H} \tilde{\mathbf{H}}_{k^*k^*}}^\perp$ for $k = 1, \dots, K$ where $k \neq k^*$
 Project orthogonally to VTC, $\tilde{\mathbf{H}}_{k^*k^*} \tilde{\mathbf{v}}_{k^*}^{l^*}$
 $\tilde{\mathbf{H}}_{kk}^\perp = \mathbf{P}_{\tilde{\mathbf{H}}_{k^*k^*} \tilde{\mathbf{v}}_{k^*}^{l^*}}^\perp \tilde{\mathbf{H}}_{kk}^\perp$ for $k = 1, \dots, K$ where $k \neq k^*$
 Compute the SVD of projected matrices
 $(\alpha_{kk} \tilde{\mathbf{H}}_{kk}^\perp) = \tilde{\mathbf{U}}_k \tilde{\mathbf{S}}_k \tilde{\mathbf{V}}_k^H$ for $k = 1, \dots, K$
 Update
 $\tilde{\mathbf{T}}_{k^*} = [\tilde{\mathbf{T}}_{k^*} \tilde{\mathbf{v}}_{k^*}^{l^*}]$
 $\tilde{\mathbf{D}}_{k^*} = [\tilde{\mathbf{D}}_{k^*} \tilde{\mathbf{u}}_{k^*}^{l^*}]$
 Output: $\tilde{\mathbf{H}}_{kk}^\perp$, $\tilde{\mathbf{V}}_k$, $\tilde{\mathbf{U}}_k$ and $\tilde{\mathbf{S}}_k$ $\forall k$; $\tilde{\mathbf{T}}_{k^*}$, $\tilde{\mathbf{D}}_{k^*}$

3.2. Stream selection procedure

The KSS algorithm selects a stream sequence from a pre-determined set of sequences of limited size. To prevent the intra-stream interference and to decrease the quantisation error, all the stream sequences include one single stream from each user. The first stream of each sequence is associated to the users having the higher SNR values. Consequently, the first stream is a pico stream because the pico users are more likely to have higher SNR values on average [15]. The construction of the stream sequences based on the regular structure is described as follows.

Each stream i can be expressed as $\pi_i = (k_i, l_i)$ where $k_i \in \{1, \dots, K\}$, $l_i \in \{1, \dots, q_{k_i}\}$ and $i \in \{1, \dots, r\}$. The set of all possible stream sequences can be defined as follows:

$$\Phi = \Phi_1 \cup \dots \cup \Phi_j \cup \dots \cup \Phi_r \quad (13)$$

where Φ_j is the set of all permutations of length $j \in \{1, \dots, r\}$ given by

$$\Phi_j = \left\{ \pi = (\pi_1 \pi_2 \dots \pi_j) \mid \forall i, i' \in \{1, \dots, j\}, \pi_i \neq \pi_{i'} \text{ if } i \neq i' \right\} \quad (14)$$

All stream sequences that include at least one stream from each BS-user pair are kept in set Π , which can be defined as follows:

$$\Pi = \left\{ \pi = (\pi_1 \pi_2 \dots \pi_j) \mid \pi \in \Phi_j; j \geq K; \forall k, \exists m \in \{1, \dots, j\} \text{ such that } k_m = k \right\} \quad (15)$$

Generated stream sequences by the proposed algorithm are kept in set Π_p , and it is defined as follows:

$$\Pi_p = \left\{ \pi = (\pi_1 \pi_2 \dots \pi_j) \mid \pi \in \Pi; j = K; l_1 = \dots = l_j = 1; k_1 \in \Gamma \right\} \quad (16)$$

For each stream sequence, streams are selected successively; the selection continues until no more streams can be selected, and all selected streams are kept in set Ψ .

Algorithm 2 performs the KSS algorithm. At the end of the algorithm, the stream sequence with the highest sum-rate is selected, so that the precoding and the postcoding matrices of the streams in the selected stream sequence are obtained.

Algorithm 2 KSS Algorithm

Input: α_{kj} , $\tilde{\mathbf{H}}_{kj}$ $\forall k, j$
 Construct the set Π_p as given in Equation (16)
for each stream sequence $\pi \in \Pi_p$ **do**
 Initialise the variables to perform selection using π
 $\Psi = \emptyset$; $\tilde{\mathbf{T}} = \emptyset$; $\tilde{\mathbf{D}} = \emptyset$; $i = 1$; $q_k = 0$ and
 $\tilde{\mathbf{H}}_{kk}^\perp = \tilde{\mathbf{H}}_{kk}$ for $k = 1, \dots, K$
 Compute the SVD of all the desired channels
 $(\alpha_{kk} \tilde{\mathbf{H}}_{kk}^\perp) = \tilde{\mathbf{U}}_k \tilde{\mathbf{S}}_k \tilde{\mathbf{V}}_k^H$ for $k = 1, \dots, K$
while $i \leq |\pi|$ **do**
 Pick the i th stream in π
 $(k^*, l^*) = \pi_i$
 Update
 $\Psi = \Psi \cup (k^*, l^*)$
 Apply **Alg. 1**
 Increment i
end while
 Calculate the sum-rate $\tilde{\mathbf{S}}\tilde{\mathbf{R}}$ for the selected streams
 Set the variables for the selected streams
 $\Psi_\pi = \Psi$
 $(\tilde{\mathbf{T}}_k)_\pi = \tilde{\mathbf{T}}_k$, $(\tilde{\mathbf{D}}_k)_\pi = \tilde{\mathbf{D}}_k$ for $k = 1, \dots, K$
end for
 Select the precoding and postcoding matrices for the permutation that maximises the sum-rate
 $\pi_p^* = \underset{\pi \in \Pi_p}{\text{argmax}} \tilde{\mathbf{S}}\tilde{\mathbf{R}}\pi$
 $\tilde{\mathbf{T}}_k = (\tilde{\mathbf{T}}_k)_{\pi_p^*}$, $\tilde{\mathbf{D}}_k = (\tilde{\mathbf{D}}_k)_{\pi_p^*}$ for $k = 1, \dots, K$
 Output: $\tilde{\mathbf{T}}_k$, $\tilde{\mathbf{D}}_k$ $\forall k$

Furthermore, the number of calls to Alg. 1 at each stream selection step of the proposed algorithm can be formulated as follows:

$$\left(\underbrace{|\Pi_p|}_{\text{Total number of stream sequences}} \times \underbrace{K}_{\text{The number of calls to Alg. 1}} \right) \quad (17)$$

4. BIT ALLOCATION METHOD

In this section, an adaptive feedback bit allocation is presented. The main objective is to maximise the average sum rate by optimising the number of bits for each user to quantify the macro and pico CDIs. Because optimising the total

number of bits for the whole system is too complex, an upper bound is obtained for the data rate of each user as defined in Equation (2). In this way, a certain number of bits to quantise the CDIs is adaptively and locally allocated at each user.

The optimisation problem of the bit allocation for KSS algorithm can be formulated for each user k as follows:

$$\max_{B_{kj}; j=1, \dots, K} \mathbb{E} [\tilde{R}_k] \quad (18a)$$

$$\begin{aligned} b &= \log_2 \left(\sum_{\substack{j=1, \\ j \neq k}}^K P_{kj} \|\mathbf{H}_{kj}\|_F^2 \left| (\tilde{\mathbf{d}}_k)^H \left(\sqrt{1-e_{kj}} \tilde{\mathbf{H}}_{kj} + \sqrt{e_{kj}} \mathbf{Z}_{kj} \right) \tilde{\mathbf{t}}_j \right|^2 \right) \\ &\leq \log_2 \left(\sum_{\substack{j=1, \\ j \neq k}}^K P_{kj} \|\mathbf{H}_{kj}\|_F^2 \left(\left| (\tilde{\mathbf{d}}_k)^H \sqrt{1-e_{kj}} \tilde{\mathbf{H}}_{kj} \tilde{\mathbf{t}}_j \right| + \left| (\tilde{\mathbf{d}}_k)^H \sqrt{e_{kj}} \mathbf{Z}_{kj} \tilde{\mathbf{t}}_j \right| \right)^2 \right) \\ &= \log_2 \left(\sum_{\substack{j=1, \\ j \neq k}}^K P_{kj} \|\mathbf{H}_{kj}\|_F^2 \left(\underbrace{(1-e_{kj}) \left| (\tilde{\mathbf{d}}_k)^H \tilde{\mathbf{H}}_{kj} \tilde{\mathbf{t}}_j \right|^2}_v + e_{kj} \left| (\tilde{\mathbf{d}}_k)^H \mathbf{Z}_{kj} \tilde{\mathbf{t}}_j \right|^2 + 2 \sqrt{1-e_{kj}} \sqrt{e_{kj}} \underbrace{\left| (\tilde{\mathbf{d}}_k)^H \tilde{\mathbf{H}}_{kj} \tilde{\mathbf{t}}_j \right| \left| (\tilde{\mathbf{d}}_k)^H \mathbf{Z}_{kj} \tilde{\mathbf{t}}_j \right|}_z \right) \right) \end{aligned} \quad (21)$$

$$\text{s.t. } \sum_{j=1}^K B_{kj} \leq B_k \quad (18b)$$

where B_{kj} represents the feedback bits allocated to the channel between the j^{th} BS and the k^{th} user, and B_k is the total number of feedback bit for the k^{th} user.

The bit allocation problem in Equation (18a) is considered for the high SINR region where $\log_2(1+x) \approx \log_2(x)$ because the interference is mitigated by performing the KSS algorithm. Furthermore, the terms of the denominator and the numerator are independently distributed random variables [25]. Therefore, $\mathbb{E} [\tilde{R}_k]$ can be rewritten by using Equation (2) as follows:

$$\begin{aligned} &\mathbb{E} \left[\log_2 \left(\frac{P_{kk} (\tilde{\mathbf{d}}_k)^H \mathbf{H}_{kk} \tilde{\mathbf{t}}_k \tilde{\mathbf{t}}_k^H \mathbf{H}_{kk}^H \tilde{\mathbf{d}}_k}{(\tilde{\mathbf{d}}_k)^H \tilde{\mathbf{B}}_k \tilde{\mathbf{d}}_k} \right) \right] \\ &= \mathbb{E} \left[\underbrace{\log_2 \left(P_{kk} (\tilde{\mathbf{d}}_k)^H \mathbf{H}_{kk} \tilde{\mathbf{t}}_k \tilde{\mathbf{t}}_k^H \mathbf{H}_{kk}^H \tilde{\mathbf{d}}_k \right)}_a \right] \\ &\quad - \mathbb{E} \left[\underbrace{\log_2 \left(\sum_{\substack{j=1, \\ j \neq k}}^K P_{kj} (\tilde{\mathbf{d}}_k)^H \mathbf{H}_{kj} \tilde{\mathbf{t}}_j \tilde{\mathbf{t}}_j^H \mathbf{H}_{kj}^H \tilde{\mathbf{d}}_k \right)}_b \right] \end{aligned} \quad (19)$$

where P_{kj} is the average received power at user k from BS j and it is calculated as $P_{kj} = P_j \alpha_{kj}^2, \forall k, \forall j$.

The first term of Equation (19) can be rewritten as follows [25]:

$$\begin{aligned} a &= \log_2 \left(P_{kk} \left| (\tilde{\mathbf{d}}_k)^H \mathbf{H}_{kk} \tilde{\mathbf{t}}_k \right|^2 \right) \\ &= \log_2 \left(P_{kk} \|\mathbf{H}_{kk}\|_F^2 \left| (\tilde{\mathbf{d}}_k)^H \left(\sqrt{1-e_{kk}} \tilde{\mathbf{H}}_{kk} + \sqrt{e_{kk}} \mathbf{Z}_{kk} \right) \tilde{\mathbf{t}}_k \right|^2 \right) \end{aligned} \quad (20)$$

Because $|x+y|^2 \leq (|x|+|y|)^2$, the second term of Equation (19), b , can be written as in Equation (21).

Assuming large number of feedback bits, the error magnitude, e_{kk} , is small, so that it can be neglected [25]. Consequently, Equation (20) can be rewritten as follows:

$$a = \log_2 \left(P_{kk} \|\mathbf{H}_{kk}\|_F^2 \left((1-e_{kk}) \left| (\tilde{\mathbf{d}}_k)^H \tilde{\mathbf{H}}_{kk} \tilde{\mathbf{t}}_k \right|^2 \right) \right) \quad (22)$$

The term $\left| (\tilde{\mathbf{d}}_k)^H \tilde{\mathbf{H}}_{kj} \tilde{\mathbf{t}}_j \right|$ can be considered approximately zero because of the IA scheme. Therefore, the terms v and z vanish and Equation (21) can be rewritten as follows:

$$b \leq \log_2 \left(\sum_{\substack{j=1, \\ j \neq k}}^K P_{kj} \|\mathbf{H}_{kj}\|_F^2 \left(e_{kj} \left| (\tilde{\mathbf{d}}_k)^H \mathbf{Z}_{kj} \tilde{\mathbf{t}}_j \right|^2 \right) \right) \quad (23)$$

Using Jensen's inequality, the upper bound for Equation (19) can be obtained as follows:

$$\begin{aligned} \mathbb{E}[a] - \mathbb{E}[b] &\leq \\ &\log_2 \left(\underbrace{\mathbb{E} \left[P_{kk} \|\mathbf{H}_{kk}\|_F^2 \left((1-e_{kk}) \left| (\tilde{\mathbf{d}}_k)^H \tilde{\mathbf{H}}_{kk} \tilde{\mathbf{t}}_k \right|^2 \right) \right]}_{T1} \right) \\ &\quad - \log_2 \left(\underbrace{\sum_{j=1, j \neq k}^K \mathbb{E} \left[P_{kj} \|\mathbf{H}_{kj}\|_F^2 \left(e_{kj} \left| (\tilde{\mathbf{d}}_k)^H \mathbf{Z}_{kj} \tilde{\mathbf{t}}_j \right|^2 \right) \right]}_{T2} \right) \end{aligned} \quad (24)$$

In Equation (24), $\mathbb{E} \left[\|\mathbf{H}_{kk}\|_F^2 \right] = N_{T_k} N_{R_k}$ [25] is determined. $T1$ in Equation (24) can be expressed as follows [26, 27]:

$$T1 = P_{kk} 2^{B_{kk}} \beta \left(2^{B_{kk}}, \frac{N_{T_k} N_{R_k}}{N_{T_k} N_{R_k} - 1} \right) \leq P_{kk} \left(1 - 2^{-\frac{B_{kk}}{N_{T_k} N_{R_k} - 1}} \right) \quad (25)$$

The second term of Equation (24), $T2$ can be expressed as follows [23, 24]:

$$T2 = P_{kj} 2^{B_{kj}} \beta \left(2^{B_{kj}}, \frac{N_{T_j} N_{R_k}}{N_{T_j} N_{R_k} - 1} \right) \leq P_{kj} 2^{-\frac{B_{kj}}{N_{T_j} N_{R_k} - 1}} \quad (26)$$

Using Equations (25) and (26) in Equation (19), the optimisation problem can be expressed as follows:

$$\max_{B_{kj}, j=1, \dots, K} \left[\log_2 \left(P_{kk} \left(1 - 2^{-\frac{B_{kk}}{N_{T_k} N_{R_k} - 1}} \right) \right) - \log_2 \left(\sum_{\substack{j=1, \\ j \neq k}}^K P_{kj} 2^{-\frac{B_{kj}}{N_{T_j} N_{R_k} - 1}} \right) \right] \quad (27)$$

$$\text{s.t. } \sum_{j=1}^K B_{kj} \leq B_k$$

Solutions for the problem expressed in Equation (27) are obtained by using an optimisation software tool [28]. After obtaining the B_{kj} values, which are real numbers, a round operation is applied to get integer values.

In order to perform the IA algorithms, each transmitter should have all the quantised CSI to obtain the precoding and the postcoding vectors [25]. Because it is achieved by the given feedback topology in Section 2.2, the optimisation problem defined in Equation (27) is also suitable for any IA algorithms such as Max-SINR or min-Leak.

5. PERFORMANCE RESULTS

The performance of the KSS algorithm is evaluated in a heterogeneous network illustrated in Figure 2. There are two transmit antennas for each pico cell and four transmit antennas for the macro cell. Each cell has one user that is randomly placed inside its coverage area. Each user has two receive antennas.

In order to study the performance results of the KSS algorithm, two different scenarios are considered. System behaviour is observed by varying the locations of the pico BSs with respect to macro BS. More precisely, pico BSs are initially placed relatively close to the macro BS, and they are shifted together with the pico users from the inner area to cell edge area of the macro BS located at (0, 0). Locations of the pico cells are identified using as the ratio

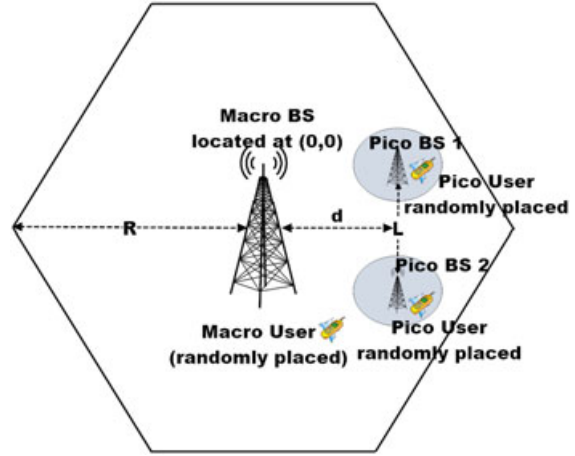


Figure 2. Scenario A: Picocells are symmetrically deployed.

Table I. System parameters.

Parameter name	Parameter value
Macro BS power	43 dBm
Pico BS power	24 dBm
Bandwidth	10 MHz
Carrier frequency	2.1 GHz
Noise power	-174 dBm/Hz
Macro cell radius	1000 m
Pico cell radius	100 m
Path loss (macro)	$128.1 + 37.6 \log_{10}(R_m(\text{km}))$ dB
Path loss (pico)	$140.7 + 36.7 \log_{10}(R_p(\text{km}))$ dB
Shadowing std. dev. (macro)	8 dB
Shadowing std. dev. (pico)	10 dB

d/R where R is the macro cell radius and d is the distance between the macro BS and each pico BS. Because, in practice, pico cells are generally deployed closer to the cell edge areas of the macro cells, we consider the ratio ranges from 0.6 to 1. In addition, the interference level between pico cells generated to each other is investigated by changing the distance between the pico cells, L , while d/R is fixed.

Simulations are carried out using the system parameters listed in Table I.

The stream sequences constructed by the KSS algorithm are illustrated in Figure 3. The selected stream sequences are initialised by the pico streams, such as the best stream of Pico 1 user is $P1_1$ and the best stream of Pico 2 user is $P2_1$. $M1_1$ is the best macro stream.

In order to analyse the behaviour of the proposed algorithm, the probability of each stream being selected as the initial stream at $d/R = 0.8$ is shown in Table II. These results are obtained by the exhaustive search that searches all possible stream combination paths and determines the stream path with the highest performance. Because it is a brute force method, it is a very complex technique. It

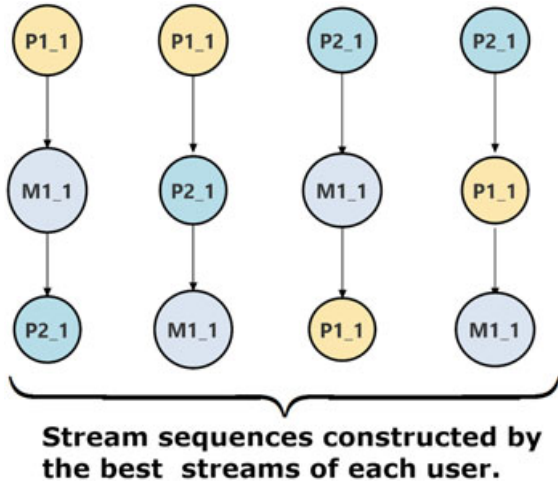


Figure 3. Stream sequences constructed by the KSS algorithm.

Table II. Probability of each stream being selected first.

d/R	Stream	Probability
0.8	M1_1	0.128
	M1_2	0.102
	P1_1	0.272
	P1_2	0.14
	P2_1	0.25
	P1_2	0.108

can be observed that the probability of selecting the first stream from the pico user is greater than selecting it from the macro user.

5.1. Scenario A

In the first scenario, pico cells are shifted towards the cell edge of the macro cell by changing the ratio d/R . The distance between the pico cells is constant, and it is $L = 150$ m.

In Figure 4, the performance comparison of different bit allocation schemes using the proposed bit allocation method is given for the total number of feedback bits $B_T = \sum_{k=1}^K B_k = 63$. In addition, the performances of the KSS algorithm and the existing iterative algorithms are compared when the perfect CSI is available at the transmitters and the receivers. The considered centralised feedback scheme explained in Section 2.2 is also the same for the iterative algorithms. All the considered algorithms are performed in the macro BS to obtain the precoding and postcoding vectors. Therefore, the feedback load is the same for both the iterative and proposed algorithms.

The proposed bit allocation method is performed for the KSS, the max-SINR [7] and the min-Leak [7] algorithms for the single stream case. It is observed that the KSS algorithm achieves higher performance for different bit

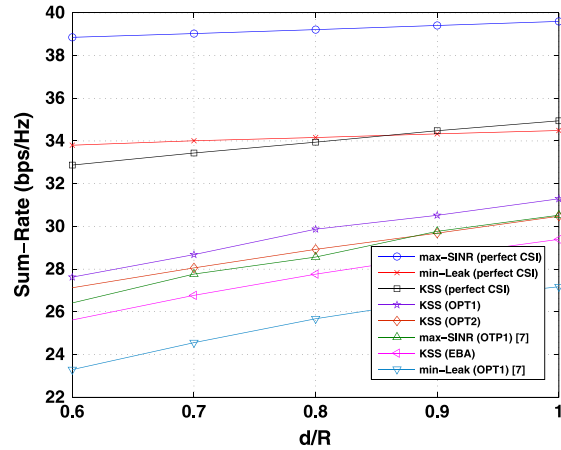


Figure 4. Scenario A: Performance comparison of the KSS algorithm and the existing algorithms for $B_T = 63$.

Table III. Scenario A: average number of allocated bits for $B_T = 63$ at $d/R = 0.8$.

$B_1 = 9$	$B_2 = 27$	$B_3 = 27$
$B_{11} = 4.76$	$B_{21} = 18.77$	$B_{31} = 18.72$
$B_{12} = 2.07$	$B_{22} = 5.42$	$B_{32} = 2.67$
$B_{13} = 2.17$	$B_{23} = 2.81$	$B_{33} = 5.51$

allocation schemes as shown in Figure 4. While, max-SINR algorithm outperforms the KSS algorithm with perfect CSI, with imperfect CSI, the KSS algorithm achieves better performance. It has been shown that the max-SINR and min-Leak algorithms are very sensitive to the imperfect CSI as demonstrated in [29, 30]. The performance degradation between the perfect CSI case and the OPT1 scheme shown in Figure 4 is approximately 4, 8.5 and 7 bps/Hz, in the KSS, max-SINR and min-Leak algorithms, respectively. Therefore, it can be observed that the KSS algorithm is less sensitive compare with the iterative algorithms.

For the limited feedback scheme, there are nine channels in Scenario A including both the desired and the interfering channels. In the equal bit allocation (EBA) scheme, the number of allocated bits to each channel is 7. It can be observed that the proposed adaptive feedback bit allocation given in Equation (27) outperforms the equal bit allocation scheme.

Using the proposed bit allocations method, different bit allocation schemes are compared for KSS algorithm by allocating different number of bits to each user, such as $B_1 = 9, B_2 = 27, B_3 = 27$ (OPT1) and $B_1 = 21, B_2 = 21, B_3 = 21$ (OPT2), and it is observed that the performance increases when more bits are allocated to the pico users. The proposed algorithm achieves approximately 1 and 4 bps/Hz gain over the max-SINR and min-Leak algorithms, respectively, for the OPT1 bit allocation scheme. The interference generated from the macro BS to pico users

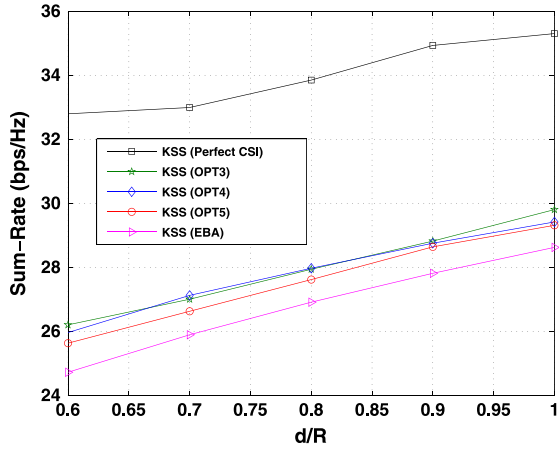


Figure 5. Scenario A: different adaptive bit allocation with $B_T = 45$ for the KSS algorithm.

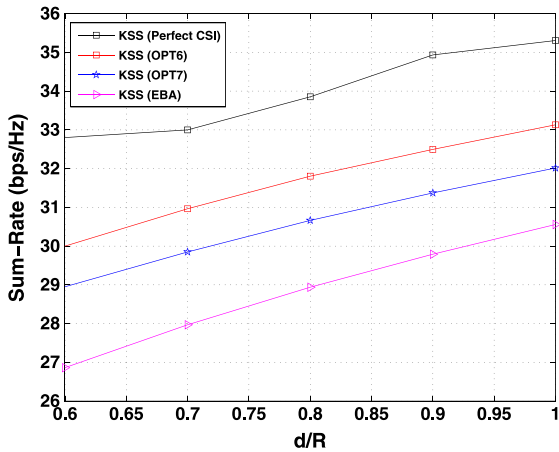


Figure 6. Scenario A: different adaptive bit allocation with $B_T = 90$ for the KSS algorithm.

is very strong, and more bits are needed to have the precise interference channels for the limited feedback. In addition, Table III shows the average number of bits allocated to each channel in detail and it is observed that the interference channels between the pico users and the macro BS need higher number of bits, B_{21} and B_{31} .

Even when the total number of feedback bits is decreased to $B_T = 45$, KSS algorithm gives better performance than the EBA scheme as given in Figure 5. In addition, different bit allocation schemes, such as $B_1 = 7, B_2 = 19, B_3 = 19$ (OPT3), $B_1 = 11, B_2 = 17, B_3 = 17$ (OPT4) and $B_1 = 15, B_2 = 15, B_3 = 15$ (OPT5) are compared for the KSS algorithm. It can be seen that OPT3 bit allocation scheme achieves better performance than OPT4 and OPT5 bit allocation schemes. In another words, similar behaviour with $B_T = 63$ is observed; that is, as the number of allocated bits increases for the pico users, the average sum rate also increases.

The comparison results for the total number of feedback bits $B_T = 90$ with different feedback schemes, such as

Table IV. Scenario A: Average Number of Allocated Bits for $B_T = 90$ at $d/R = 0.8$.

$B_1 = 10$	$B_2 = 40$	$B_3 = 40$
$B_{11} = 4.85$	$B_{21} = 30.07$	$B_{31} = 29.82$
$B_{12} = 2.49$	$B_{22} = 5.63$	$B_{32} = 4.43$
$B_{13} = 2.66$	$B_{23} = 4.30$	$B_{33} = 5.75$

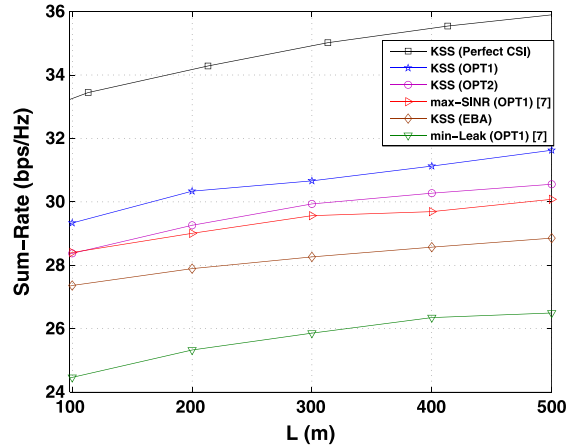


Figure 7. Scenario B: Performance comparison of the KSS algorithm and the existing algorithms for different bit allocation schemes with $B_T = 63$.

such as $B_1 = 10, B_2 = 40, B_3 = 40$ (OPT6) and $B_1 = 30, B_2 = 30, B_3 = 30$ (OPT7) are given in Figure 6. Even the increased total number of feedback bits, it is observed that allocating higher number of feedback bits to the pico cells gives better performances as shown in Figure 6. Allocating more bits for B_{21} and B_{31} is important to handle the interference generated from the macro BS to the pico users, as also seen in Table IV, which gives the average number of allocated bits for each channel considering the case $B_T = 90$.

5.2. Scenario B

In this scenario, pico cells are shifted away from each other along the y-axis while the x-axis is fixed. The distance between the pico cells, L , varies between 100m and 500m.

The performance results obtained with $B_T = 63$ are given for OPT1 and OPT2 bit allocation schemes in Figure 7. Once again, the results indicate that the interference generated from macro BS to pico users is very dominant. Moreover, the KSS algorithm achieves higher sum-rate than the existing iterative IA algorithms and the performance of the proposed solution for the adaptive bit allocation scheme is higher than the equal bit allocation scheme.

For the greater total number of bits, the performance comparison is given in Figure 8 with different bit allocation schemes to each user, such as OPT6 and OPT7. It can be seen again that it is critical to handle the interference

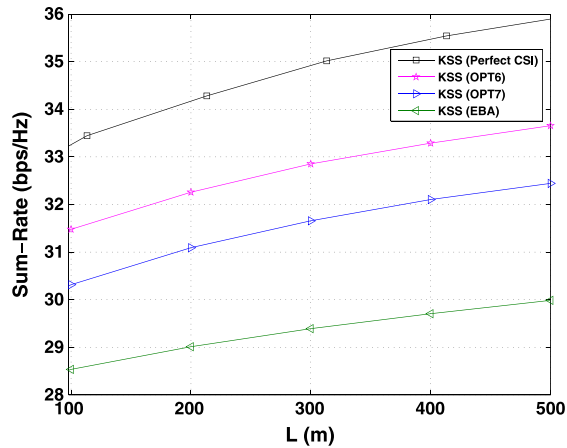


Figure 8. Scenario B: different adaptive bit allocation with $B_T = 90$ for the KSS algorithm.

generated from macro BS to pico users by allocating more bits to the interference channels between the macro BS and pico users.

The structures of the proposed and the iterative algorithms are completely different. The proposed algorithm is a successive algorithm while max-SINR and min-Leak algorithms are iterative algorithms. Therefore, the comparison of the complexities of these algorithms is not straightforward. Indeed, there is a trade-off between the performance and the complexity for the iterative algorithms. The required number of the iterations increases in the high SNR regions for the iterative algorithms while the number of calls to Alg.1 does not change with different SNR values in the proposed algorithm. The complexity of the proposed algorithm can be calculated using Equation (17), and it is 12 for Scenario A and Scenario B.

6. CONCLUSION

In this study, we have proposed the KSS algorithm for the limited feedback schemes in the heterogeneous networks, and an adaptive bit allocation has been presented to reduce the quantisation error on the proposed algorithm. Because the intra-stream interference has a severe impact on the performance of the IA with the limited feedback schemes, the proposed algorithm selects only one stream from each user. Furthermore, the streams of the pico cells are initially selected in order to reduce the interference coming from the macro cell to the pico cell, and it is also supported by the statistical analysis gathered from the exhaustive search.

The interference between the selected streams is handled by performing orthogonal projections after selecting each stream. The precoders and postcoders have been obtained using the quantised CDI.

The presented adaptive bit allocation scheme has been performed for two different scenarios for the heterogeneous networks. The number of bits of each user is opti-

mised for the CDI feedback to maximise the average sum rate of the network.

The performance of the proposed algorithm has been evaluated by varying the positions of pico BSs. Simulation results demonstrate that the proposed algorithm achieves higher performance gain when compared with the existing IA algorithms with the limited feedback scheme. It has been shown that the presented adaptive bit allocation scheme improves the system throughput compared with the equal bit allocation. Furthermore, it has been observed that most of the bits should be allocated to the interference channels between the macro BS and pico users because the generated interference from the macro BS to the pico users is very dominant.

REFERENCES

1. Tao H, Guoqiang M, Qiang L, Lijun W, Jing Z. Interference minimization in 5G heterogeneous networks. *MONET* 2015; **20**(6): 756–762.
2. Zhang H, Chen S, Li X, Ji H, Du X. Interference management for heterogeneous networks with spectral efficiency improvement. *IEEE Wireless Communications* 2015; **22**(2): 101–107.
3. Damnjanovic A, Montojo J, Wei Y, Ji Y, Luo T, Vajapeyam M, *et al.* A survey on 3GPP heterogeneous networks. *IEEE Wireless Communications* 2011; **18**(3): 10–21.
4. Zheng Z, Dowhuszko AA, Hämäläinen J. Interference management for LTE-advanced Het-Nets: stochastic scheduling approach in frequency domain. *Trans Emerging Telecommunications Technologies* 2013; **24**(1): 4–17.
5. Jafar SA. Interference alignment: a new look at signal dimensions in a communication network. *Foundations and Trends in Communications and Information Theory* 2011; **7**(1): 1–136.
6. Cadambe VR, Jafar SA. Interference alignment and degrees of freedom of the K-User interference channel. *IEEE Transactions on Information Theory* 2008; **54**(8): 3425–3441.
7. Gomadam K, Cadambe VR, Jafar SA. A distributed numerical approach to interference alignment and applications to wireless interference networks. *IEEE Transactions on Information Theory* 2011; **57**(6): 3309–3322.
8. Amara M, Pischella M, Le Ruyet D. Enhanced stream selection for sum-rate maximization on the interference channel. In *International Symposium on Wireless Communication Systems (ISWCS), Paris*, 2012; 151–155.
9. Suh C, Ho M, Tse DNC. Downlink interference alignment. *IEEE Transactions on Communications* 2011; **59**(9): 2616–2626.
10. Ruan L, Lau VKN, Rao X. Interference alignment for partially connected MIMO cellular networks.

- IEEE Transactions on Signal Processing* 2012; **60**(7): 3692–3701.
11. Guillaud M, Gesbert D. Interference alignment in the partially connected K-User MIMO interference channel. In *European Signal Processing Conference (EUSIPCO), Barcelona*, 2011; 1095–1099.
 12. Shin W, Noh W, Jang K, Choi HC. Hierarchical interference alignment for downlink heterogeneous networks. *IEEE Transactions on Wireless Communications* 2012; **11**(12): 4549–4559.
 13. Liu G, Sheng M, Wang X, Jiao W, Li Y, Li J. Interference alignment for partially connected downlink MIMO heterogeneous networks. *IEEE Transactions on Communications* 2015; **63**(2): 551–564.
 14. Aycan E, Özbek B, Le Ruyet D. Hierarchical successive stream selection for heterogeneous network interference. In *IEEE Wireless Communications and Networking Conference (WCNC), Istanbul*, 2014; 1143–1148.
 15. Aycan E, Özbek B, Le Ruyet D. On stream selection for interference alignment in heterogeneous networks. *EURASIP Journal on Wireless Communications and Networking* 2016; **2016**: 1–18.
 16. Love DJ, Heath RW, Lau VKN, Gesbert D, Rao BD, Andrews M. An overview of limited feedback in wireless communication systems. *IEEE Journal on Selected Areas in Communications* 2008; **26**(8): 1341–1365.
 17. Özbek B, Le Ruyet D. *Feedback Strategies for Wireless Communication Systems*, Springer-engineering Series Book. Springer Science Business Media: New York, U.S.A, 2013.
 18. Aycan E, Özbek B, Le Ruyet D. Improved Successive Stream Selection with Quantized Channel in Heterogeneous Networks. In *International Symposium on Wireless Communication Systems (ISWCS)*, Belgium, 2015; 1–5.
 19. Chen X, Yuen C. Performance analysis and optimization for interference alignment over MIMO interference channels with limited feedback. *IEEE Transactions on Signal Processing* 2014; **62**(7): 1785–1795.
 20. Cho S, Huang K, Kim DK, Lau VKN, Chae H, Seo H, *et al.* Feedback-topology Designs for interference alignment in MIMO interference channels. *IEEE Transactions on Signal Processing* 2012; **60**(12): 6561–6575.
 21. Rihan M, Elsabrouty M, Muta O, Furukawa H. Interference Alignment with Limited Feedback for Macrocell-Femtocell Heterogeneous Networks. In *IEEE Vehicular Technology Conference (VTC)*, Glasgow, 2015; 1–5.
 22. Niu Q, Zeng Z, Zhang T, Gao Q, Sun S. Interference alignment and bit allocation in heterogeneous networks with limited feedback. In *IEEE International Symposium on Wireless Personal Multimedia Communications (WPMC)*, Sydney, NSW, 2014; 514–519.
 23. Ravindran N, Jindal N. Limited feedback-based block diagonalization for the MIMO broadcast channel. *IEEE Journal on Selected Areas in Communications* 2008; **26**(8): 1473–1482.
 24. Jindal N. MIMO broadcast channels with finite-rate feedback. *IEEE Transactions on Information Theory* 2006; **52**(11): 5045–5060.
 25. Anand K, Gunawan E, Guan YL. Beamformer design for the MIMO interference channels under limited channel feedback. *IEEE Transactions on Communications* 2013; **61**(8): 3246–3258.
 26. Zhang J, Andrews JG. Adaptive spatial intercell interference cancellation in multicell wireless networks. *IEEE Journal on Selected Areas in Communications* 2010; **28**(9): 1455–1468.
 27. Özbek B, Le Ruyet D. Adaptive limited feedback links for cooperative multi-antenna multicell networks. *EURASIP Journal on Wireless Communications and Networking* 2014; **2014**: 1–11.
 28. Grant M, Boyd S. *CVX: Matlab software for disciplined convex programming, version 2.1*, 2014. Available from: <http://cvxr.com/cvx> [accessed on September 2015].
 29. Xie B, Li Y, Minn H, Nosratinia A. Adaptive interference alignment with CSI uncertainty. *IEEE Transactions on Communications* 2013; **61**(2): 792–801.
 30. Razavi SM, Ratnarajah T. Performance analysis of interference alignment under CSI mismatch. *IEEE Transactions on Vehicular Technology* 2014; **63**(9): 4740–4748.